LAGRANGIAN MODELLING OF EXTREME WAVE GROUPS

E. V. Buldakov; Department of Civil Engineering, UCL, Gower Street, LONDON, WC1E 6BT, UK

SUMMARY

A 2D Lagrangian numerical wave model is presented and validated against a set of physical wave-flume experiments on focussed wave groups. The Lagrangian calculations demonstrate good agreement with experimental results. The model proves to be efficient in modelling both long-term wave propagation along the flume and strongly-nonlinear waves including initial stages of wave breaking.

1 INTRODUCTION

Numerical simulation of extreme ocean waves implies contradicting requirements to a model. It should be capable of both accurate modelling of long-term propagation of a dispersive wave and adequate representation of behaviour of strongly-nonlinear waves including wave breaking. The main difficulty of numerical solvers for modelling of extreme waves is strong deformation the computational domain. There are different ways of dealing with this problem. The most powerful models for simulation of strongly-nonlinear and breaking waves are based on a volume of fluid (VoF) method (e.g. de Jouëtte *et al.*, 1996). These models use a larger computational domain with cells not occupied by the fluid and introduce an artificial variable describing occupation of a cell. The boundary between fluid and air domains is not specified exactly but smoothed over several grid cells, which leads to considerable errors in the dispersion relation. Together with high requirements for computational resources this makes using VoF methods for modelling long-term processes impractical. The natural way of modelling strong deformations of a fluid domain is using equations of fluid motion in the Lagrangian form which though in some cases are more complicated than the Eulerian counterparts, to be solved in a fixed domain of Lagrangian labels. Lagrangian models are capable of efficient modelling of very steep and overturning waves and still have advantages for long-term runs since they follow water surface and produce smaller error in the dispersion relation. Some of the contemporary solvers use mixed approaches utilising certain elements of the Lagrangian description but they still do not exploit all its advantages. Mixed-Eulerian-Lagrangian (MEL) boundary-integral Boundary-integral methods (Longuet-Higgins & Cokelet, 1976; Tsai & Yue, 1996) use the linearity of inviscid irrotational Eulerian formulation and can not be used for flows with arbitrary vorticity. The smooth particle hydrodynamics (SPH) approach (e.g. Monaghan, 1994) though can be considered as fully Lagrangian is based on the artificial physical models and has no such a firm theoretical background as the straightforward numerical solution of Lagrangian equations. Surprisingly, the author could not find many published works where the fully-Lagrangian formulation would be used for solving water-waves problems. The rare example is the work of Protopopov (2007) who uses the formal transformation to Lagrangian coordinates for 2D Euler equations, suggests a numerical method for solving the resulting problem and applies it to selected free surface flows. In this paper the finite-difference technique is applied directly to Lagrangian equations of fluid motion. A 2D version of the inviscid finite difference Lagrangian numerical solver is introduced and applied for modelling of wave groups generated in a wave flume. By the complexity level the considered technique is comparable with potential Eulerian solvers and far simpler then SPH or VoF methods.

2 LAGRANGIAN 2D WATER-WAVE FORMULATION

We use a 2D inviscid fully-Lagrangian water-wave formulation presented in Buldakov *et al.* (2006) describing time evolution of Cartesian coordinates of fluid particles $x(a,c,t)$ and $z(a,c,t)$ as functions of Lagrangian labels (a,c). The formulation includes the Lagrangian continuity equation and the Lagrangian form of vorticity conservation

$$\frac{\partial(x,z)}{\partial(a,c)} = J(a,c)\,; \quad \frac{\partial(x_t,x)}{\partial(a,c)} + \frac{\partial(z_t,z)}{\partial(a,c)} = \Omega(a,c)\,, \tag{1}$$

and the dynamic free-surface condition

$$x_{tt}x_a + z_{tt}z_a + g\,z_a\,\big|_{c=0} = 0\,. \tag{2}$$

Functions $J(a,c)$ and $\Omega(a,c)$ are given functions of Lagrangian coordinates. $J(a,c)$ is defined by initial positions of fluid particles associated with labels (a,c). If initial positions of fluid particles are used as Lagrangian labels then $J=1$. $\Omega(a,c)$ gives the vorticity distribution and for an irrotational flow $\Omega=0$. Lagrangian formulation does not require the kinematic free-surface condition which is satisfied by specifying a fixed curve in the Lagrangian coordinates corresponding to the free surface, e.g. $c=0$. A specific problem within the general formulation is defined by boundary and initial conditions. Conditions describing a wave flume used in this paper are specified as follows. We use the rectangular Lagrangian domain with $c=0$ being the free surface and $c=-h$ being the bottom. The known shape of the bottom provides the condition on the lower boundary of the Lagrangian domain For the case of a flat bed of depth h we have $z=-h$. On the right boundary of the

Lagrangian domain $a = a_{\max}$ a given motion of a vertical wall represents the motion of a piston wavemaker: $x(a_{\max}, c, t) = a_{\max} + X_{\rm wm}(t)$, where $X_{\rm wm}(t)$ is a prescribed motion of the paddle, and we have a solid vertical wall on the left boundary $x(a_{\min}) = a_{\min}$. Positions and velocities of fluid particles must be supplied as initial conditions, e.g. still water conditions.

3 NUMERICAL MODEL

The problem formulated in the previous section is solved numerically using a finite-difference technique. Since equations (1) for internal points of the domain include only first order spatial derivatives a compact four-point Keller box scheme can be used for finite-difference approximation of these equations. Values of unknown functions x and z on the sides of the stencil box are calculated as averages of values at adjacent points and then used to approximate derivatives across the box by first-order differences. The scheme provides the second-order approximation for the central point and uses only 4 mesh points in the corners of the box which makes the resulting solver less demanding for memory resources. Time derivatives in (1) are approximated by second-order backward differences. Spatial derivatives in the free-surface boundary condition (2) are approximated by second-order central differences and special attention must be paid to approximation of second time derivatives since it defines the form of the numerical dispersion relation and is crucial for the overall stability of the scheme. For simplicity let us consider a case of continuous spatial field in (1-2) combined with discrete time approximation in (2). Let us approximate second derivatives by 3-point backward differences and expand this approximation to Taylor series with respect to a small time step τ. We get

$$(f(t-2\,\tau) - 2\,f(t-\tau) + f(t))/\tau^2 = f''(t) - \tau\,f'''(t) + O(\tau^2)\,. \tag{3}$$

The approximation is of the first order with the leading term of the error proportional to the third derivative of a function, which gives the main contribution to the error of the dispersion relation. Under an assumption of small perturbations we represent unknown functions in the form $x = a + \varepsilon\,\xi(a,c,t)$; $\quad z = c + \varepsilon\,\zeta(a,c,t)$ and keep only linear terms of expansions with respect to the small displacement amplitude $\varepsilon \to 0$. Introducing a displacement potential ϕ: $\eta = \partial\phi/\partial a$; $\quad \zeta = \partial\phi/\partial c$ we satisfy the vorticity conservation to the first order and the corresponding approximation of the continuity equation is the Laplace equation for ϕ. The dynamic surface condition (2) becomes

$$\phi_a'' + g\,\phi_{ac} - \tau\,{\phi_a}''' = O(\tau^2)\,, \tag{4}$$

where dashes denote time derivatives and only the leading term of the approximation error from (3) is taken into account. To derive the numerical dispersion relation we are looking for a solution in the form of a regular wave in deep water: $\phi = e^{i\,k\,a}\,e^{k\,c}\,e^{i\,\omega\,t}$, which satisfy the Laplace equation. The dynamic condition (4) is satisfied when a dispersion relation connecting ω and k is valid. Similar analysis can be performed for higher orders of approximation of the derivatives. Below is the summary of dispersion relations obtained for orders $n = 1 \ldots 4$:

$$\omega = \sqrt{gk}\,(\,\pm 1 + \tfrac{1}{2}\,i\,\hat\tau + O(\hat\tau^2)\,)\,; \qquad \omega = \sqrt{gk}\,(\pm 1 \mp \tfrac{11}{24}\,\hat\tau^2 + \tfrac{1}{2}\,i\,\hat\tau^3 + O(\hat\tau^4)\,)\,;$$
$$\omega = \sqrt{gk}\,(\,\pm 1 - \tfrac{5}{12}\,i\,\hat\tau^3 + O(\hat\tau^4)\,)\,; \quad \omega = \sqrt{gk}\,(\,\pm 1 \pm \tfrac{137}{360}\,\hat\tau^4 - \tfrac{19}{24}\,i\,\hat\tau^5 + O(\hat\tau^6)\,)\,.$$

Here we use a non-dimensional expansion parameter $\hat\tau = \sqrt{gk}\,\tau$. As can be seen, the first-order scheme (top left) introduces numerical viscosity proportional to $\hat\tau$ which leads to fast decay of perturbations and is not acceptable for long-term modelling. The higher-order schemes (second row) include terms proportional to $-i$, leading to grows of perturbations and making the numerical scheme unstable. We therefore use the second-order scheme (top right), which incorporates a numerical error to dispersion at the second order $\hat\tau^2$ and weak dissipation at the third order $\hat\tau^3$. The overall numerical scheme is therefore of the second order in both time and space.

A fully-implicit time marching is applied, and Newton iterations are used on each time step to solve nonlinear algebraic difference equations. To reduce calculation time the inversion of a Jacobi matrix during Newton iterations is made at a first iteration and when iterations start to diverge. Otherwise the previously calculated inverse Jacobi matrix is used. Usually only one inversion per each time step is required. An adaptive mesh is used in the horizontal direction with an algorithm based on the shape of the free surface in Lagrangian coordinates $z(a,0,t)$ to refine mesh at each time step in regions of high surface gradients and curvatures. Constant mesh refinement near the free surface is used in the vertical direction Convergence tests were performed for some of the cases. The scheme demonstrate convergence for all parameters: number of computational points in horizontal and vertical directions and time step. Compromising between accuracy and computational resources we use 201×21 computational mesh and 0.002 sec time step for most calculations in the paper, which required about 5 sec of computational time of a standard PC for each time step. For highly-nonlinear stages of flow with development of wave breaking a higher number of spacial points and a smaller time step were used.

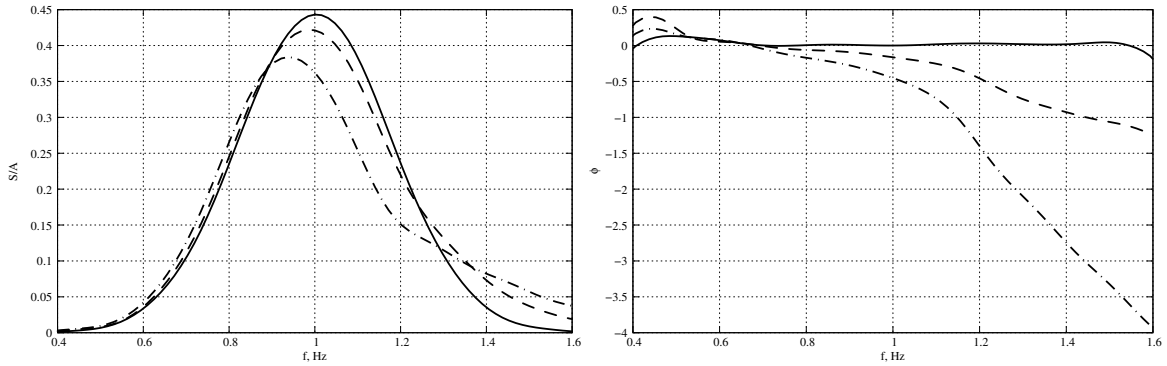

Figure 1: Linearised spectra of experimental wave groups at a focus point. Amplitude (left) and phase (right). Solid– $A = 2.5\,cm$; dashed– $A = 5\,cm$; dash-dotted– $A = 7.5\,cm$.

4 EXPERIMENTS

Experiments on generation and propagation of focussed wave groups were performed in a coastal wave flume of the Civil Engineering department at UCL. The flume has the width of $45\,cm$ and the length of the working section between two piston wavemakers is $12.5\,m$. A paddle on the right end of the flume is used as a wave generator and the opposite paddle as an absorber. Center of the flume is used as an origin of the coordinate system with the x-axis directed towards the wave generator positioned at $x = 6.25\,m$. Water depth over a horizontal bed of the flume was set to $h = 40\,cm$. The flume paddle uses a control system operating in frequency domain with force feedback which allows precise control and partial absorption of reflected waves. Input of the control system is the linearised amplitude spectrum of the generated wave at the center of the flume. The control system uses discrete spectrum and generates periodic paddle motions. For our experiments we use an overall return period of $64\,sec$, which is the time between repeating identical events produced by the paddle. Wave propagation was monitored by a series of resistance wave probes measuring surface elevation. Motion of the paddle had also been recorded. Each of experimental runs included 6 return periods. It was assumed that the periodic wave system with the return period of $64\,sec$ is established in the flume after the first period. The data for the first return period was neglected and the rest of the data was averaged between the following 5 periods. Each of the runs was repeated at least 3 times at and high level of repeatability was demonstrated. For each spectrum two waves with constant phase shift of π were generated: peak and through focussed waves. The corresponding data records were used for harmonic analysis of signals. Even harmonics were found as a half-sum of peak and trough focussed signals, and odd harmonics as their half difference (Taylor *et al.*, 2004). The dominating part of the odd-harmonic signal is due to a linear part of the spectrum. The form and the amplitude of the linearised spectrum completely define the wave. Our aim is therefore generating wave groups with a prescribed linearised spectrum focussed at $x = 0$. Paddle control does not account for dissipative and nonlinear effects, and a spectrum of an actually generated wave group differs from an input spectrum of the control system. We use the following iterative procedure to generate waves of desired spectrum focussed at the center of the flume:

$$a^n_{\rm in}(\omega) = a^{n-1}_{\rm in}(\omega)\, a_{\rm tgt}(\omega)/a^{n-1}_{\rm out}(\omega); \quad \phi^n_{\rm in}(\omega) = \phi^{n-1}_{\rm in}(\omega) + \left(\, \phi_{\rm tgt}(\omega) - \phi^{n-1}_{\rm out}(\omega)\,\right), \tag{5}$$

where $a^n_{\rm in}(\omega)$ and $\phi^n_{\rm in}(\omega)$ are input amplitude and phase of the spectral component at frequency ω for iteration n; $a^n_{\rm out}(\omega)$, $\phi^n_{\rm out}(\omega)$ are amplitudes and phases of the corresponding spectral components of a linearised spectrum of a generated wave at the center of the flume (focus point), and $a_{\rm tgt}(\omega)$, $\phi_{\rm tgt}(\omega)$ are target spectral components. We applied the iterative procedure (5) to generate a Gaussian wave group with peak frequency of $1\,Hz$ focussed at the center of the flume and having linear focus amplitude of $2.5\,cm$. Then we use the same input spectrum to generate higher amplitude waves with linear focus amplitudes A of 5 and $7.5\,cm$. The resulting waves are of tree distinct types: weakly non-linear, moderately non-linear and strongly non-linear breaking waves. Their linearised spectra at $x = 0$ are shown on figure 1. As can be expected, non-linear defocussing and transformation of linear spectrum can be observed for higher amplitude waves.

5 RESULTS

The numerical Lagrangian model introduced in Sections 2,3 have been used to simulate wave flume experiments described in the previous section. Parameters of calculations correspond to experimental parameters and linearised experimental records of motion of a wave generator had been used to generate waves in the numerical wave flume. Figure 2 demonstrates the excellent comparison between experimental and computational results for amplitude spectrum and time history of surface elevation at the focus point $x = 0$ for a moderately steep

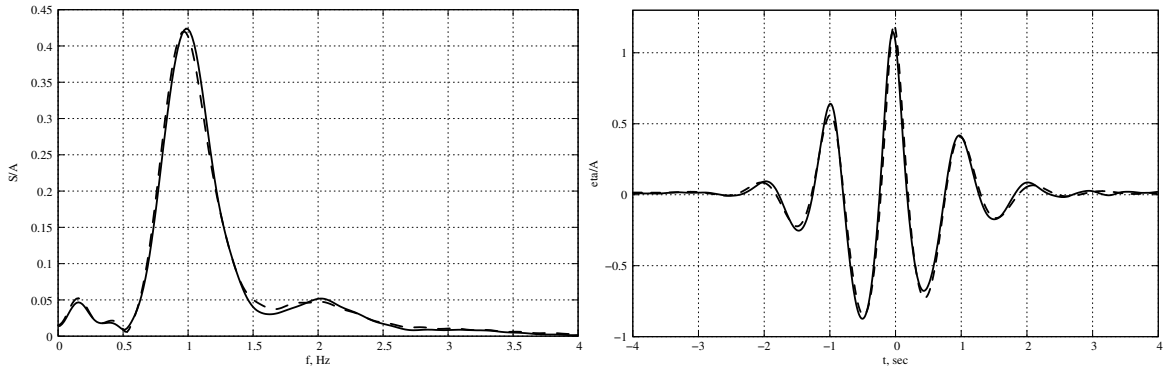

Figure 2: Comparison of experimental (solid) and calculated (dashed) results for surface elevation at $x = 0$ for a wave group with $A = 5\,cm$. Left– full amplitude spectrum; right– time history.

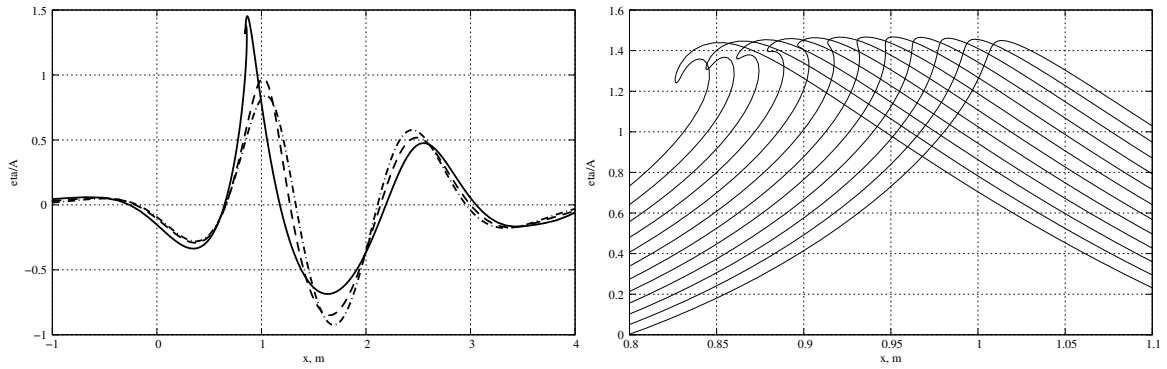

Figure 3: Left: wave profiles for wave groups of different amplitudes at $t = -1.7\,sec$. Right: development of a micro-plunger at the crest of a breaking wave starting from $t = -1.8\,sec$, time between profiles is $0.01\,sec$.

wave of $A = 5\,cm$. Wave generation process starts approximately $10\,sec$ before the linear focus time $t = 0$ and the distance between the focus point and the wave generator is $6.25\,m$. We therefore can see that the model is capable of adequate modelling of propagation of nonlinear dispersive waves for time scales of several periods and length scales of several wave lengths. For a high amplitude wave ($A = 7.5\,cm$) wave breaking was observed in the experiment. Modelling of spilling breaking is beyond the capability of the current version of the Lagrangian solver and the computational process for this wave breaks down at $t \approx -1.7\,sec$. However, as can be seen from Figure 3 the model generates a realistic near-breaking profile with developing a micro-plunger at the wave crest. These results can give valuable information on kinematics of pre-breaking wave which can be used for calculating loads of such waves on structures. To conclude, the Lagrangian numerical model provides a powerful and effective tool for modelling strongly-nonlinear waves. The model demonstrates good agreement with experiments. It is efficient in modelling both long-term wave propagation along the flume and developing of extreme waves including initial stages of wave breaking.

References

Buldakov, E. V., Eatock Taylor, R. & Taylor, P. H. 2006 New asymptotic description of nonlinear water waves in Lagrangian coordinates. *J. Fluid Mech.* **562**, 431–444.

Longuet-Higgins, M. S. & Cokelet, E. D. 1976 The deformation of steep surface waves on water. I. A numerical method of computation. *Proc. R. Soc. Lond. A.* **350**, 1–26.

de Jouëtte, C., Gouez, J. M. L., Put, O. & Rigaud, S. 1996 Volume of fluid method (VOF) applied to non-linear wave problems on body-fitted grids. In *11th International Workshop on Water Waves and Floating Bodies*. Hamburg, Germany.

Monaghan, J. J. 1994 Simulating free surface flows with SPH. *Journal of Computational Physics* **110**, 399–406.

Protopopov, B. E. 2007 Computation of wave motions of fluid using euler's equations. *Computational Technologies* **12** (1), 82–92, (in Russian).

Taylor, P., Hunt, A., Borthwick, A. & P.K.Stansby 2004 Phase inversion and the identification of harmonic structure in costal engineering experiments. In *29th International Conference on Coastal Engineering*. Lisbon, Portugal.

Tsai, W. & Yue, D. K. P. 1996 Computation of nonlinear free-surface flows. *Ann. Rev. Fluid Mech.* **28**, 249–278.